

Synthesis of Magnetron-Sputtered TiN Thin-Films on Fiber Structures for Pulsed-Laser Emission and Refractive-Index Sensing Applications at 1550nm

Omar Gaspar Ramírez ¹, Manuel García Méndez ² * Ricardo Iván Álvarez Tamayo ³, and Patricia Prieto Cortés ⁴

¹ Postgraduate Program, Faculty of Physics and Mathematics, Universidad Autónoma de Nuevo León, San Nicolás de los Garza 66455, México

² Faculty of Physics and Mathematics, Universidad Autónoma de Nuevo León, San Nicolás de los Garza 66455, México

³ Faculty of Mechatronics, Bionics and Aerospace, Universidad Popular Autónoma del Estado de Puebla, Puebla 72410, México

⁴ Benemérita Universidad Autónoma de Puebla, Puebla, 72000, México

* Correspondence: manuel.garciamnd@uanl.edu.mx (M.G.M.)

Deposition of thin films: RF and DC equipments.

Figure 15 shows the image of the RF equipment, with which the Ti nitride-films of 1st batch were grown. With the RF equipment, a single optical fiber was mounted onto a glass substrate as a template, for a total of three single-fiber/substrate. These samples were labeled F01, F02 and F03, using a TiN target. Their respective template-substrates were similarly named for XPS and UV-Vis characterization. Additionally, with other experimental conditions, Ti and TiN targets were used to grow the films of 2nd batch. In this case, two optical fibers were mounted per substrate, for a total of two double-fiber/substrate. Fibers were named F04 and F05 and the substrate-template F0405, for XPS and UV-Vis characterization, using the Ti target. Finally, fibers were named F06 and F07 and the substrate-template F0607, for XPS and UV-Vis characterization, using the TiN target.

At the right, an image of the optical fibers mounted on substrate after deposition is included. In this case, corresponds to fibers F04 and F05, from Ti target. It is noteworthy its yellowish color, characteristic of TiN. These optical fibers were characterized for saturable absorber application.

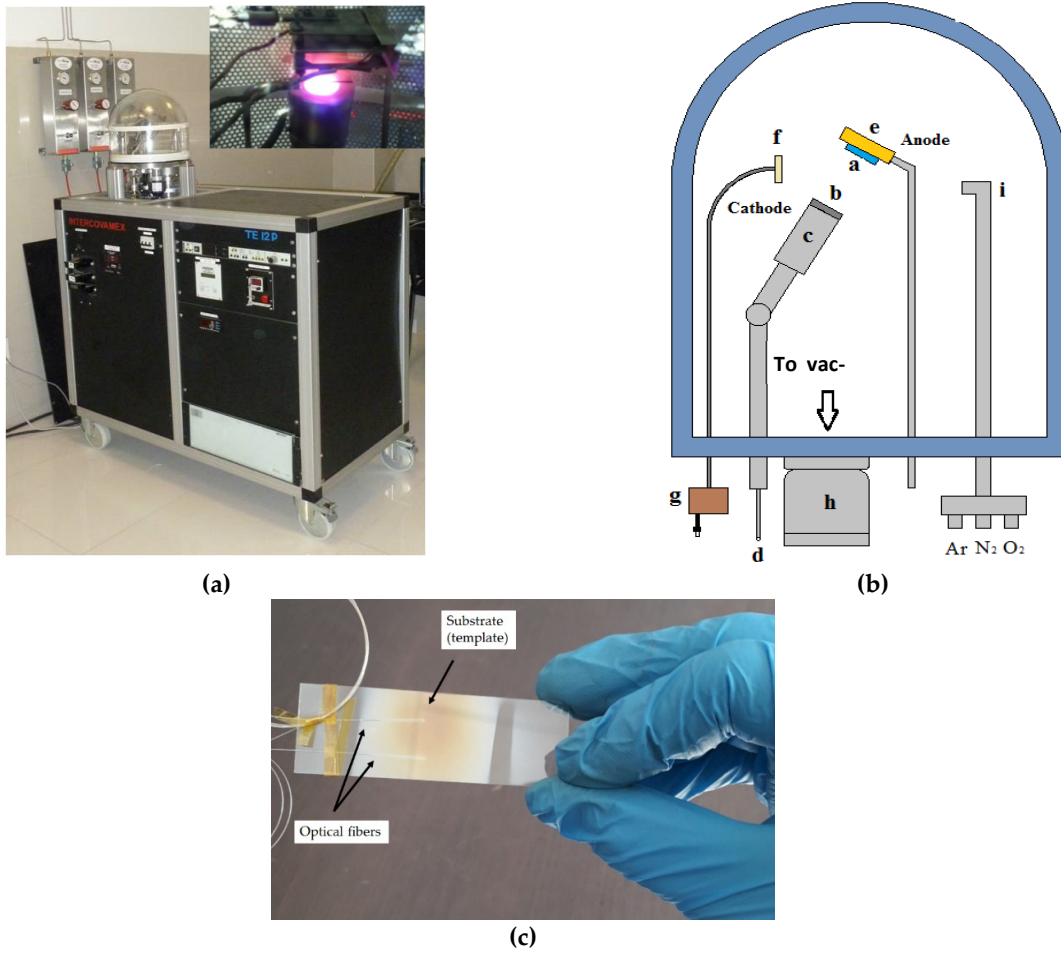


Figure S1. (a) Sputtering system for RF deposition, (b) Schematic detail of the deposition chamber: a—Substrate, b—Target holder, c—Magnetron, d—RF source connection e—substrate holder and heating source, f—Quartz sensor, g—USB connection to computer for measuring deposition rate, h—Mechanical-turbomolecular vacuum-pumps system, i—High purity gas-inlet, (c) TiN sample deposited onto the optical fiber attached to glass substrate.

Figure 16 shows the image of the DC equipment, with which the oxynitride films were grown. This optical fiber was characterized for LMR refractometer application.

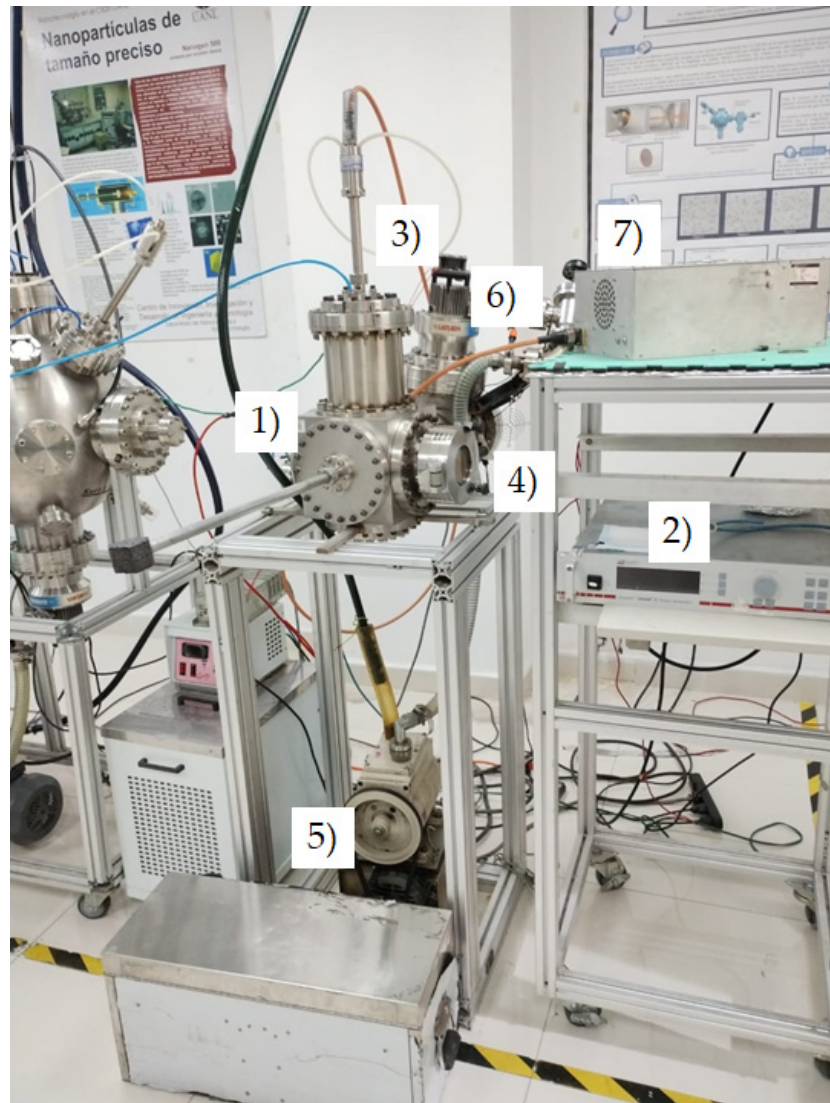


Figure S2. Sputtering system for DC deposition: 1—deposition chamber, 2—RF source, 3—magnetron, 4—Introduction chamber, 5—Mechanical pump, 6—Turbomolecular pump, 7—RF generator.

Procedure to obtain the bang gap from Tauc's curve

The procedure to obtain the E_g from Tauc's curves is described in steps as follows:

1. A transmittance spectra is obtained from UV-Vis spectroscopy.
2. With the thickness, the absorption coefficient, α , is obtained using the Formula 1.
3. Using the Formula 2, for a direct transition ($r = 2$), a curve of $(\alpha h\nu)^2$ vs E is constructed (Tauc's curve).
4. A theoretical sigmoidal curved is applied for fitting the Tauc's curve (Origin® software).
5. From theoretical curve, the 2nd derivative is obtained, and it results in two inflection points.
6. The region containing the inflection points is the zone of linearization.
7. The E_g is obtained from line extrapolation.

This procedure was applied systematically to avoid ambiguities in extrapolation that would arise if experimental points alone were used to trace a line. Figure 17 displays the experimental and theoretical curves, highlighting the inflection points and the zone of linear extrapolation.

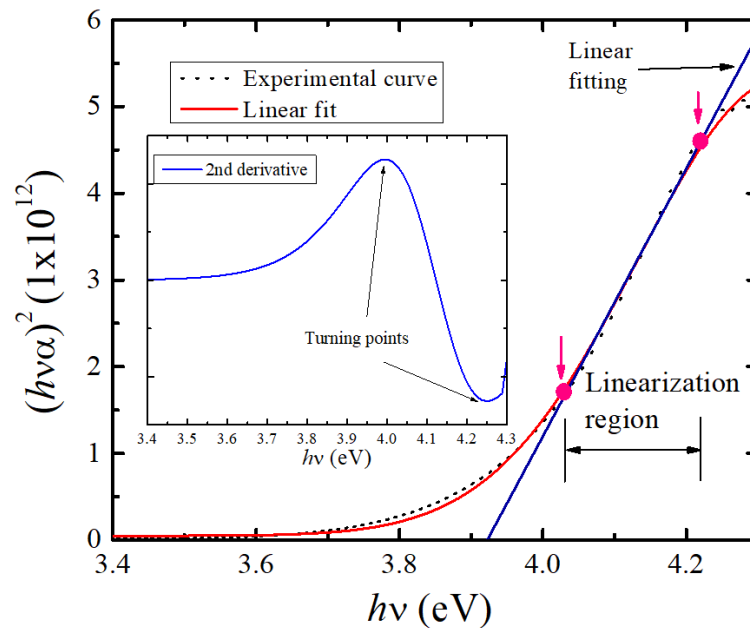


Figure S3. Tauc's curve with the procedure used to obtain E_g .

XPS analysis of Ti and TiN targets.

In order to obtain more information and determination of elemental and chemical states, XPS characterization of Ti and TiN targets, used in our deposition process, was performed. Below in Figure 18 is included a photograph of such targets.



Figure S4. (a) Ti target (b) TiN target.

Figure 19 displays the XPS spectra corresponding to the TiN target. Before deposition, target surface shows the presence of oxides, as observed for Ti window, with oxide and nitride states, together with the characteristic oxide satellite. Also, it is notorious the presence of N, which is expected in this target. After deposition, it appears the signal of Ti in nitride state. Its expected characteristic shape is very different from the one of metallic Ti (BE $2p_{3/2}$ at 454.3 eV). In this case, the $2p_{1/2}$ and $2p_{3/2}$ transitions appear more asymmetric because satellite features. Thus, differences in BE and shape allows to detect and distinguish between metallic, nitride and oxide states. In photograph, target appears to be bright yellowish, as expected for TiN.

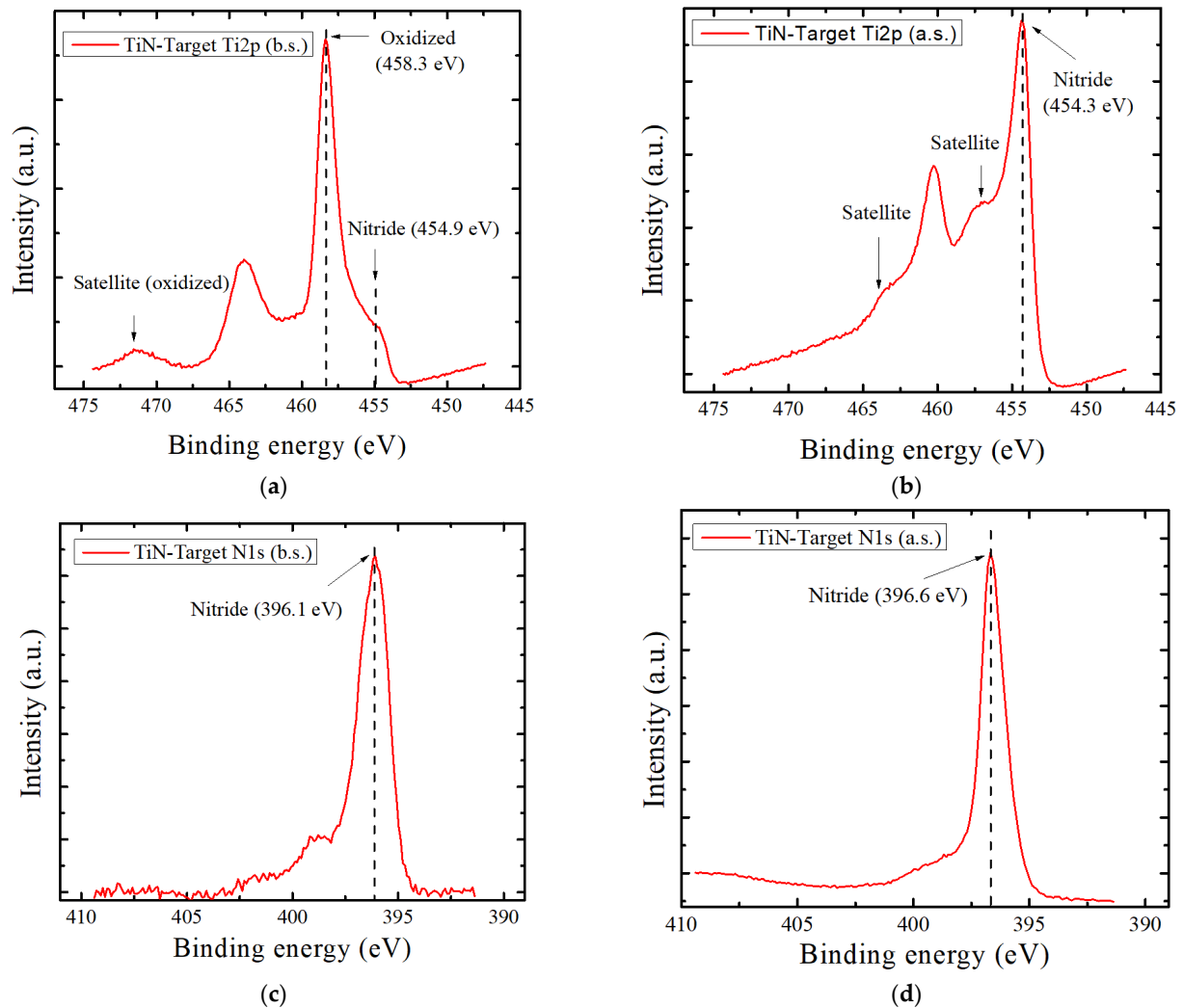


Figure S5. XPS spectra for the Ti2p and N1s high resolution windows for TiN target. (a) and (c) before deposition. (b) and (d) after deposition.

Figure 20 displays the XPS spectra corresponding to the Ti target. Before deposition, target surface shows the presence of oxides. Before sputtering is observed the satellite, characteristic of Ti oxides, which vanishes after sputtering. Also, it is notorious the presence of N, which evidence that the sputtering process, due to the deposition process, led to the target nitridation. After deposition, Ti in metallic is observed, with its expected characteristic shape. BE of metallic state (Ti2p3/2 at 453.3 eV) and its characteristic shape were not detected in our samples. Also, it can be observed that some nitridation remains after deposition. In photograph, target appears to be somewhat yellowish, and no silverfish as expected for metallic Ti.

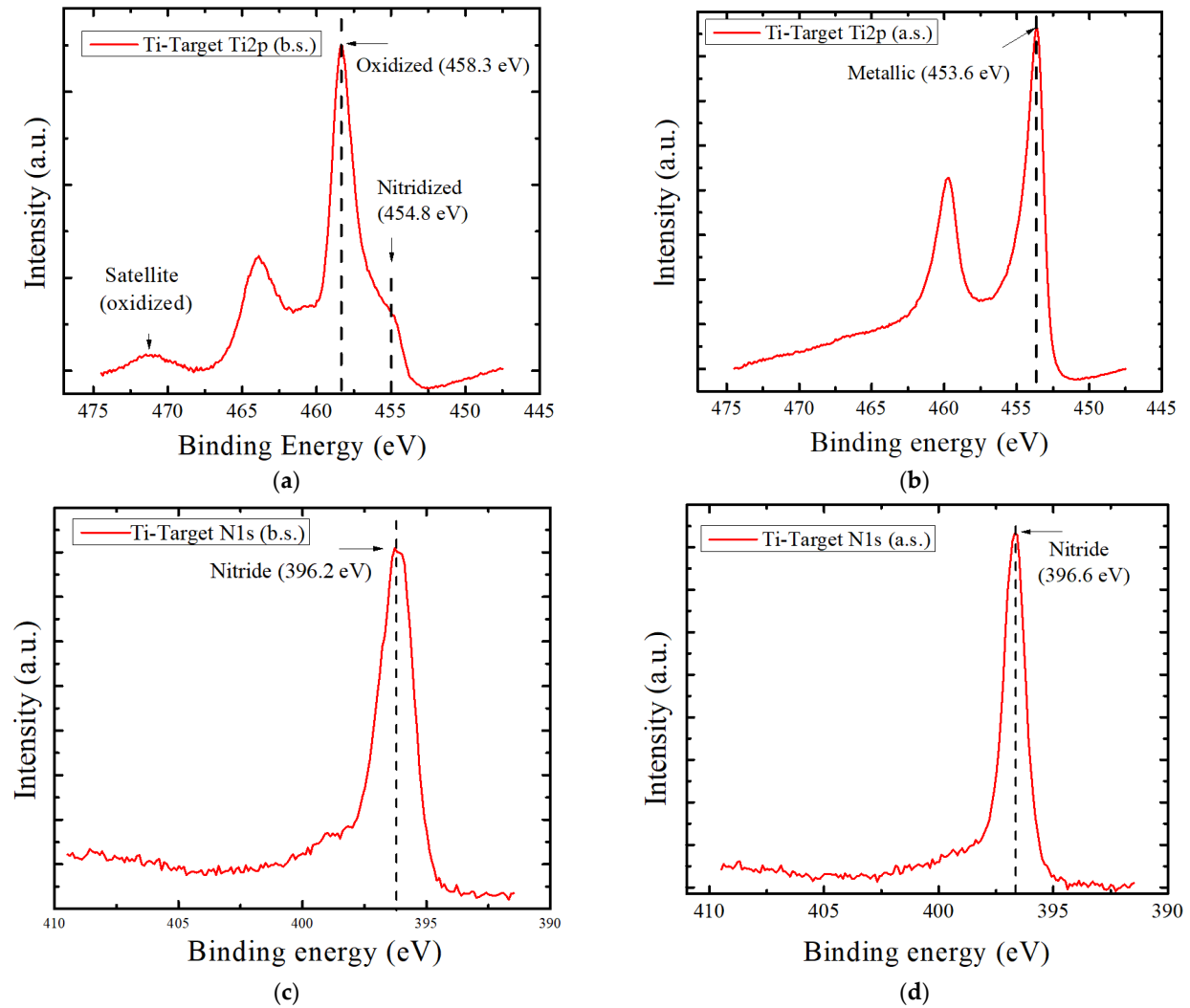


Figure S6. XPS spectra for the Ti2p and N1s high resolution windows for Ti target. (a) and (c) before deposition. (b) and (d) after deposition.